Hindawi
International Journal of Antennas and Propagation
Volume 2024, Article ID 9326275, 7 pages
https://doi.org/10.1155/2024/9326275

Research Article

A Simultaneous Study on Wire-Loop, Plate-Loop, and Plate Antennas for Wideband Circular Polarization

Kazuhide Hirose,[1] **Mitsuki Hirose**,[1] **and Hisamatsu Nakano**[2]

[1]*College of Engineering, Shibaura Institute of Technology, Tokyo 135-8548, Japan*
[2]*Science and Engineering, Hosei University, Tokyo 184-8548, Japan*

Correspondence should be addressed to Kazuhide Hirose; khirose@sic.shibaura-it.ac.jp

Received 8 November 2023; Revised 20 December 2023; Accepted 4 May 2024; Published 11 May 2024

Academic Editor: Rakesh Chowdhury

We investigate three square-shaped antennas to increase the bandwidth of circular polarization. Each antenna has two adjacent corners excited with the same amplitudes and a phase difference of 90° using a branched feedline vertical to the ground plane. We evaluate the 3 dB axial ratio bandwidth as a function of the loop-arm width using the moment method. It is found that the axial ratio bandwidth reaches 38% for an arm width of 0.04 wavelengths, wider than that of a wire-loop antenna by a factor of three. The simulated results are verified by experimental ones.

1. Introduction

A loop antenna above the ground plane radiates a circularly polarized (CP) wave [1–7]. The CP radiation is obtained using a perturbation segment [1–4] or loop-shaped deformation [5–7]. A novel loop antenna without an additional segment or shape deformation has recently been proposed [8]. The antenna is excited using a branched feedline vertical to the ground plane (see Figure 1(a)) and exhibits the widest CP wave bandwidth among the loop antennas.

This paper aims to increase the CP wave bandwidth of a loop antenna with a vertical, branched feedline. We transform the wire loop into a plate one and eventually into a plate antenna by increasing the arm width of the loop (see Figures 1(b)–1(d)). The CP wave bandwidth versus loop arm width is evaluated using the moment method [9].

The working mechanism lies in the following facts for three antennas with a single feed [5]: discrete concentric triple-, connected concentric triple-, and plate-loop antennas, each with the same perimeter and antenna arm width. (1) The discrete triple loop exhibits triple-band characteristics, i.e., three minima in the frequency response of the axial ratio. (2) Unlike the discrete loop, the connected triple loop exhibits a wideband frequency response of the axial ratio similar to the plate loop. These facts encourage one to expect an increase in the axial ratio bandwidth when transforming a wire loop into a plate loop. Note that the study in [5] discusses CP radiation with an axial ratio bandwidth of up to 4% and does not refer to a plate antenna.

This is the first simultaneous study of three resonant radiation elements, i.e., wire-loop, plate-loop, and plate antennas. Consequently, we find a plate loop with a maximum 3 dB axial ratio bandwidth of 38%, which is three times wider than that of a wire loop [8]. It is emphasized that this bandwidth is still wider than those of nonresonant elements, such as a compact spiral above the ground plane (23%) [10].

In this paper, we numerically investigate three square-shaped antennas. Subsequently, the numerical results are validated with experimental ones and compared with those of similar studies. Finally, we summarize the results in the conclusion.

2. Numerical Methods and Results

Figure 1 shows the square wire-loop, plate-loop, and plate antennas. Each antenna with side length L is located at a height h above the ground plane. The two corners F_n ($n = 1$ and 2) are connected to a vertical, branched feedline

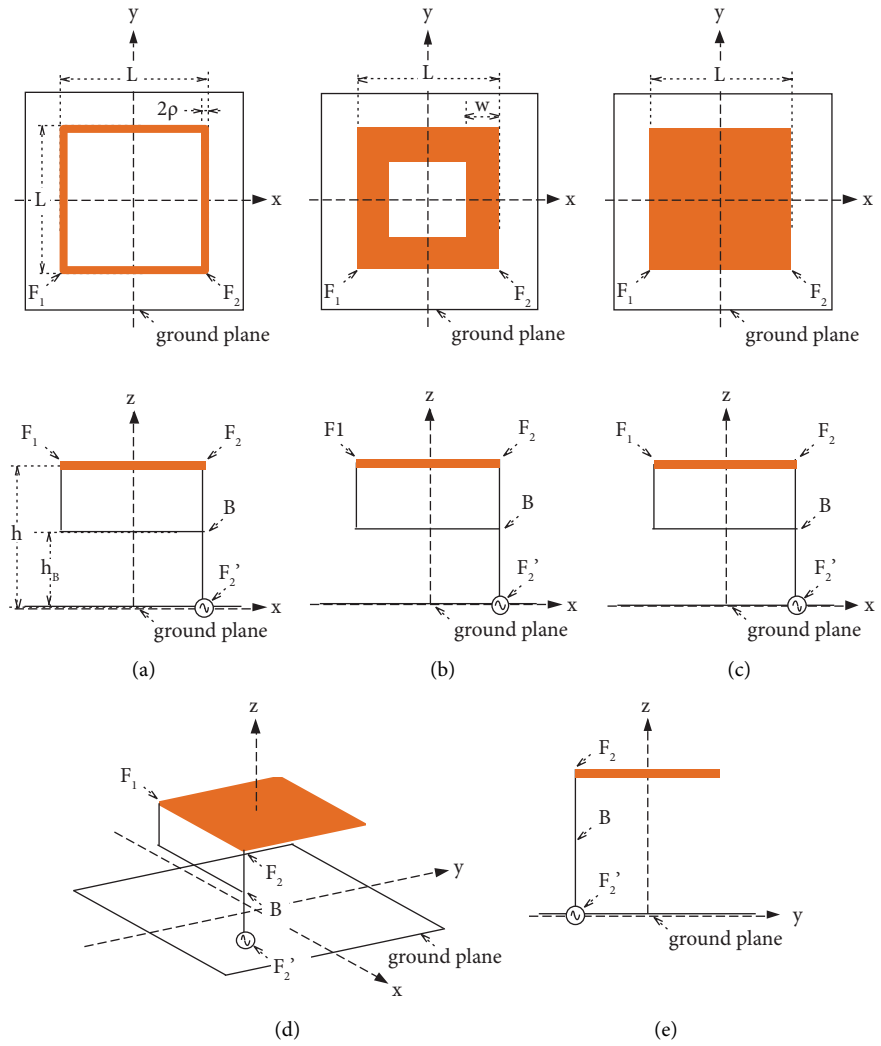

Figure 1: Antennas with a branched feedline $F_n - B - F_2'$ ($n = 1$ and 2) vertical to the ground plane. (a) Wire-loop antenna [8]. (b) Plate-loop antenna. (c) Plate antenna. (d) Perspective view of the plate antenna. (e) Side view of the plate antenna in the y-z plane.

$F_n - B - F_2'$, and the bottom end F_2' is excited by a coaxial line. The height of branch point B is designated as h_B. The antenna is composed of wires of radius ρ, and a wire-grid model [11] is used to form the plate.

The antenna is analyzed using our developed computer program based on the moment method [9]. The flowchart for the computer program is shown in Figure 2, where radiation characteristics are calculated using the current distribution determined by the moment method. The ground plane size is assumed to be infinite and the image theory is used. The side length L and branch-point height h_B are selected for CP radiation. The other parameters are fixed at $(h,\ \rho) = (\lambda_0/4,\ \lambda_0/200)$ [8], where λ_0 is the free-space wavelength at a test frequency f_0.

The simulated CP wave bandwidths of the plate loop and the plate antennas are depicted in Figure 3. A 3 dB axial ratio bandwidth is evaluated versus the loop-arm width w. At each point w, the $(L,\ h_B)$ parameters are optimized for CP radiation. It is found that the bandwidth becomes a maximum value at $w = 0.04\lambda_0$ with $(L,\ h_B) = (0.27\lambda_0,\ 0.11\lambda_0)$. The value is 38%, which is three times as wide as that (12%) of a wire-loop antenna [8]. Based on this result, the loop-arm width is fixed at $w = 0.04\lambda_0$ throughout this paper.

Figure 4(a) shows the simulated radiation patterns of the plate loop antenna. The radiation is decomposed into right- and left-hand CP wave components. It is observed that the antenna radiates a CP beam normal to the antenna plane in the $+z$-axis direction. The average half-power beamwidth (HPBW) in the $\phi = 0^\circ$ and 90° planes is 90°. Figure 4(b) shows the results for the wire-loop antenna. It is seen that the antenna radiates a CP beam similar to that of the plate-loop one. The average HPBW is 85°.

The solid line in Figure 5 shows the gain versus frequency for the plate-loop antenna combined with the axial ratio. The 3 dB gain drop bandwidth from the peak value is 38% $(0.93 f_0$–$1.37 f_0)$, where the axial ratio is less than 3 dB. For comparison, the dotted lines show the results for the wire-loop antenna. It is observed that the plate-loop antenna has

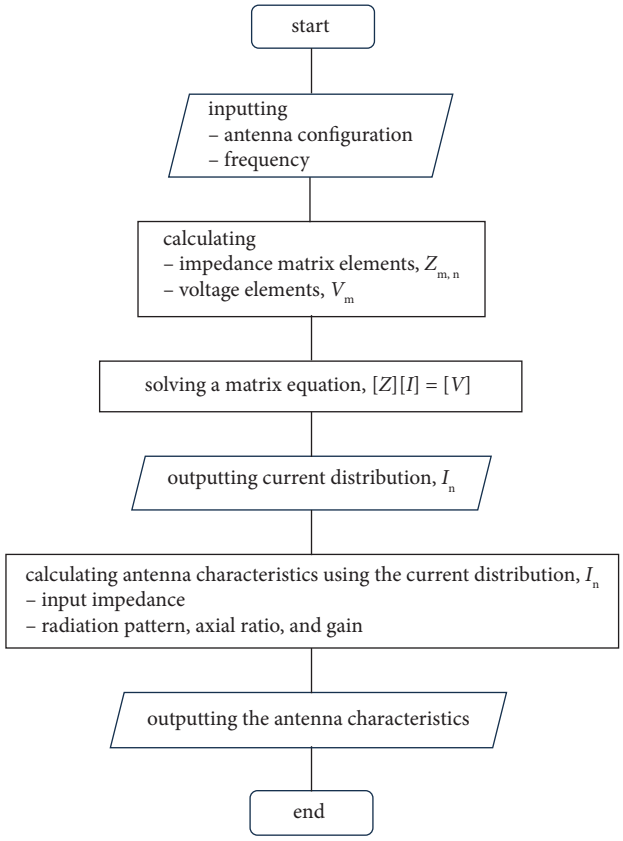

Figure 2: Flowchart for a computer program.

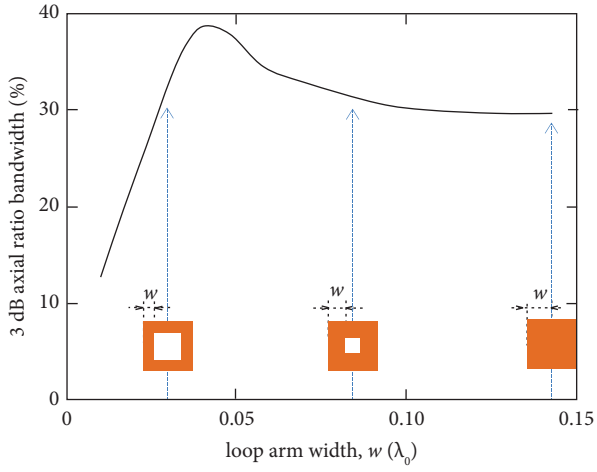

Figure 3: Simulated CP wave bandwidths of plate-loop and plate antennas versus loop arm width.

a maximum gain (7.1 dBi), which is comparable to that of the wire-loop antenna (7.5 dBi).

3. Experimental Results

Further consideration is given to the impedance matching of the plate-loop antenna. For this, the straight feedline B-F_2' shown in Figures 1(b) and 1(e) is modified to a crank one, as shown in the inset of Figure 6. We select the crank parameters (ℓ_1, ℓ_2) while keeping the other configuration parameters the same as those in Section 2.

The solid line in the upper part of Figure 6 shows the simulated VSWR versus frequency for (ℓ_1, ℓ_2) = ($0.02\lambda_0$, $0.20\lambda_0$), with the gain and axial ratio shown in the lower figure. The VSWR is evaluated for a 75 Ω coaxial line. It is found that the 3 dB gain drop bandwidth is 36% ($0.94f_0$–$1.35f_0$), where the VSWR and axial ratio are less than 2 and 3 dB, respectively.

The simulated radiation patterns for (ℓ_1, ℓ_2) = ($0.02\lambda_0$, $0.20\lambda_0$) are shown with solid and dotted lines in Figure 7. The radiation patterns are almost the same as those for the straight feedline B-F_2' (see Figure 4(a)). The average HPBW is 87°, and the gain is 7.3 dBi.

Until this point, the radiation characteristics have been discussed using the simulated results. These results are experimentally validated using an antenna fabricated at $f_0 = 3$ GHz with a ground plane of $5\lambda_0 \times 5\lambda_0$. Photographs of the antenna are shown in Figure 8. The small circles and dots in Figures 6 and 7 show the experimental results. They agree with the simulated results. There is a deviation between the experimental and simulated axial ratios. The deviation is attributed to the incompleteness of the hand-made prototype in comparison with the simulated antenna configuration.

Finally, we compare our results with those of similar studies. The comparisons are presented in Table 1. It can be said that the present antenna has the widest axial ratio bandwidth. The widest bandwidth is owing to the loop-arm width selected for wideband CP radiation, as shown in Figure 3.

It is necessary to describe the practical aspects of the present plate loop antenna. The antenna can be applied in series-fed [12, 13] and dual-element [14, 15] arrays with a simple feeding system. The array antennas have been designed using a wire loop with a branched feedline vertical to the ground plane. Therefore, replacing the wire loop with the present plate one in future work could expand the axial ratio bandwidth of the array antennas.

Before concluding, we explain the mechanism behind an expansion in the axial ratio bandwidth shown in Figure 3. As mentioned in Section 1, the working mechanism lies in frequency responses of the axial ratios of three antennas with a single feed above the ground plane [5]: discrete concentric triple-, connected concentric triple-, and plate-loop antennas, as shown in Figure 9. The dotted lines show three minima at f_n frequencies ($n = 1, 2, 3$) for the discrete concentric triple-loop antenna, and each bandwidth is almost the same as that of a single-loop antenna with the same side length (L) and height above the ground plane. Once the three loops in the discrete triple antenna are connected, the connected triple antenna has a wideband CP radiation, as shown with a dashed line. It should be noted that the plate-loop antenna exhibits almost the same result as the connected triple antenna, as shown with a solid line. This fact implies that the plate-loop antenna can be considered the connected triple-loop antenna. In summary, a plate-loop antenna corresponds to a connected concentric triple-loop antenna with a wider axial ratio bandwidth than a single-loop antenna.

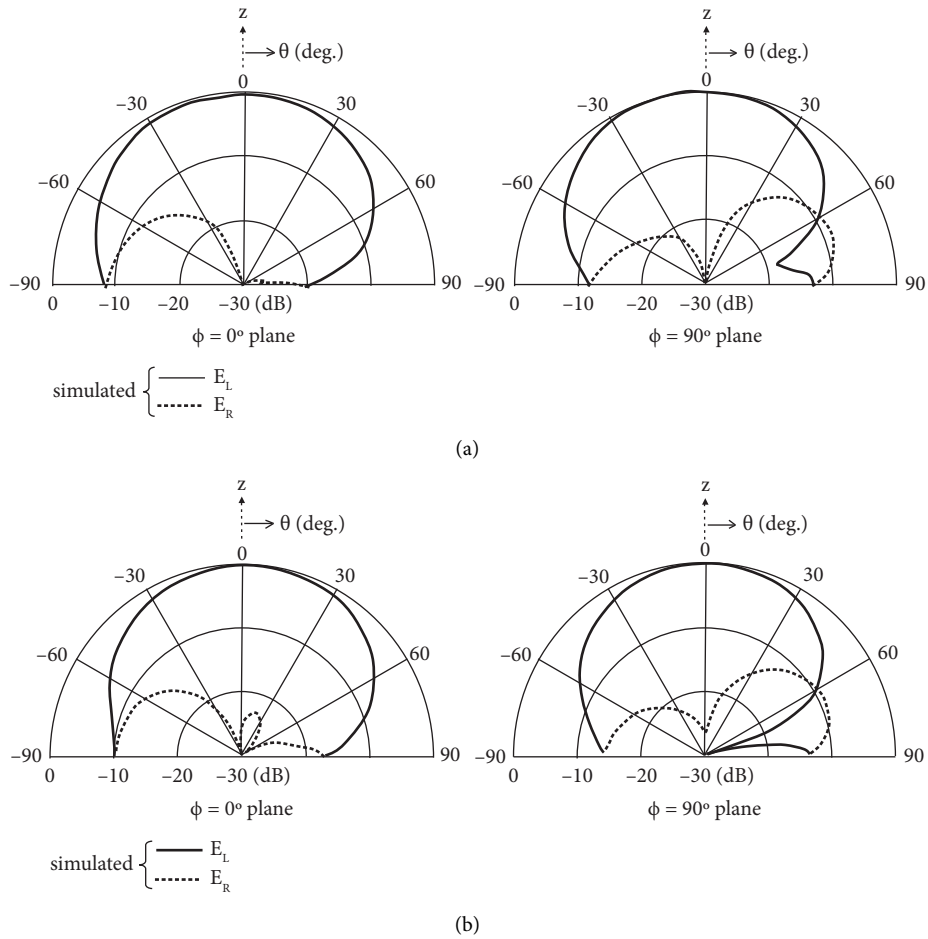

Figure 4: Simulated radiation patterns. (a) Plate-loop antenna with $w = 0.04\lambda_0$. (b) Wire-loop antenna [8].

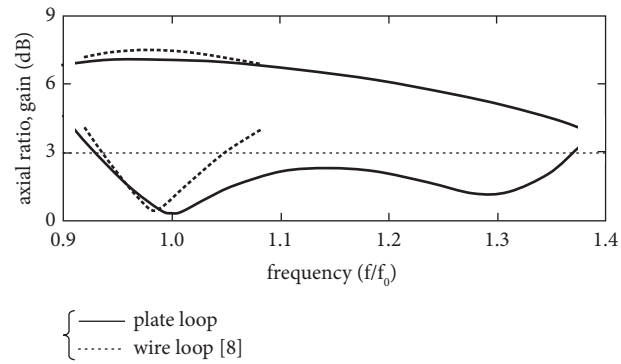

Figure 5: Simulated frequency responses of the axial ratio and gain of plate- and wire-loop antennas.

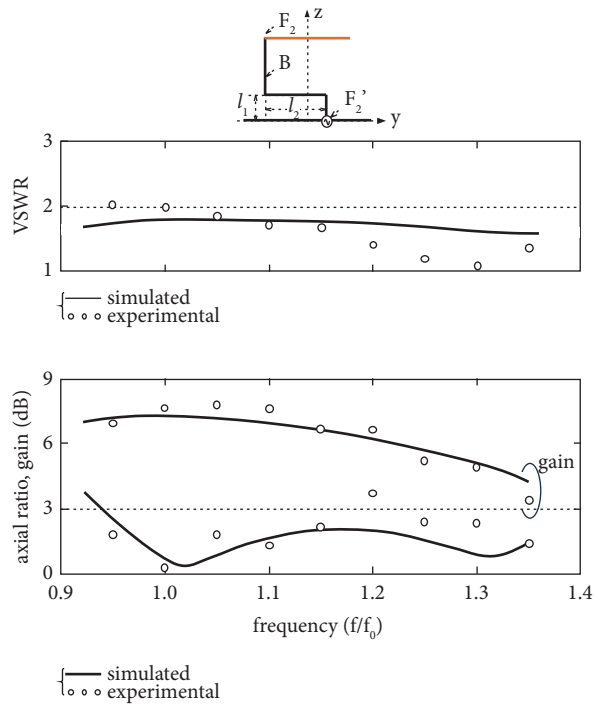

Figure 6: Frequency responses of VSWR, gain, and axial ratio of a plate-loop antenna with a crank feedline B-F_2'.

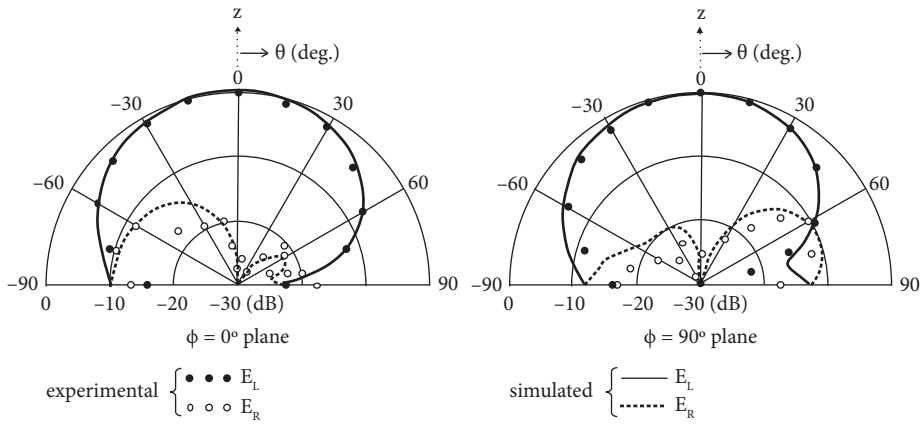

Figure 7: Radiation patterns of a plate-loop antenna with a crank feedline B-F_2'.

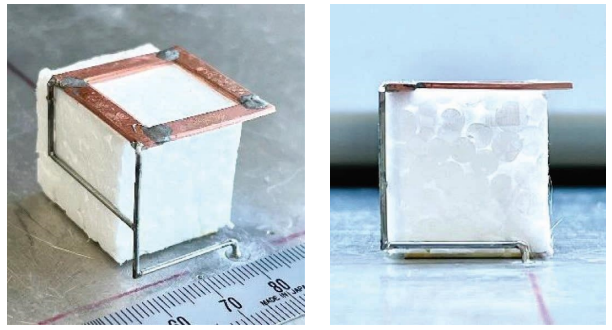

(a) (b)

Figure 8: Photographs of a plate-loop antenna with a crank feedline B-F_2'. (a) Perspective view. (b) Side view.

Table 1: Comparison with other studies.

Study	Loop shape	Method for circular polarization	ARBW (%)	OLBW (%)	Gain (dBi)	Fre (GHz)
[1]	Square	Perturbation segment	1.02	1.02	7.6	1.57
[2]	Circular		12.7	12.7	7~8	2.5
[5]	Hexagonal	Loop-shaped deformation	4.0	4.0	—	—
[7]	Rectangular		4	—	9.1	1.5
Present	Square	Vertical, branched feedline	39	36	7.3	3

ARBW: 3 dB axial ratio bandwidth; OLBW: overlapped bandwidth for ARBW, 3 dB gain-drop bandwidth, and bandwidth of VSWR <2; Fre: frequency; –: not described.

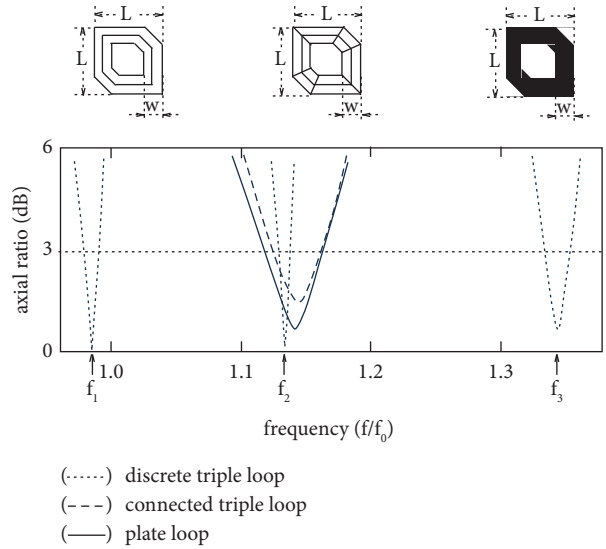

Figure 9: Axial ratio versus frequency for three loop antennas with a single feed [5]. Note that the antennas have the same perimeter ($4L$) and antenna-arm width (w) at the same height above the ground plane.

4. Conclusions

We have studied three resonant radiation elements with a branched feedline vertical to the ground plane. We select the branch-point height and square-side length for CP radiation, and the 3 dB axial ratio bandwidth is evaluated versus the loop-arm width w. It is found that a plate-loop antenna with $w = 0.04\lambda_0$ has a 3 dB gain drop bandwidth of 36%, where the axial ratio and VSWR are less than 3 dB and 2, respectively. It is emphasized that the resultant bandwidth is wider than those of nonresonant elements, such as a compact spiral antenna.

Data Availability

The numerical and experimental data used to support the findings of this study are included within the article.

Conflicts of Interest

The authors declare that they have no conflicts of interest.

Acknowledgments

The authors thank Wiley's English language service and MDPI's English editing service for preparing this manuscript.

References

[1] T. Han, C. Sim, and C. Chen, "A circularly polarized meander loop antenna design for GNSS Application," *IEEE Antennas and Wireless Propagation Letters*, vol. 20, no. 12, pp. 2235–2239, 2021.

[2] L. Zhang, S. Gao, Q. Luo, P. Young, and Q. Li, "Wideband loop antenna with electronically switchable circular polarization," *IEEE Antennas and Wireless Propagation Letters*, vol. 16, pp. 242–245, 2017.

[3] J. Liu, B. Zeng, L. Badjie et al., "Single-feed circularly polarized aperture-coupled stack antenna with dual-mode square loop radiator," *IEEE Antennas and Wireless Propagation Letters*, vol. 9, pp. 887–890, 2010.

[4] R. Li, J. Laskar, and M. M. Tentzeris, "Broadband circularly polarized rectangular loop antenna with impedance matching," *IEEE Microwave and Wireless Components Letters*, vol. 16, no. 1, pp. 52–54, 2006.

[5] K. Hirose, H. Nakagawa, and H. Nakano, "A square loop antenna modified for circular polarization— in application to multiband and wideband antennas," in *Proceedings of the European Conference on Antennas and Propagation, EuCAP*, Davos, Switzerland, April 2016.

[6] Y. Zhang and L. Zhu, "Printed dual spiral-loop wire antenna for broadband circular polarization," *IEEE Transactions on Antennas and Propagation*, vol. 54, no. 1, pp. 284–288, 2006.

[7] Y. Murakami, T. Nakamura, A. Yoshida, and K. Ieda, "Rectangular loop antenna for circular polarization," *IEICE Transactions*, vol. 78, pp. 520–527, 1995.

[8] K. Hirose, S. Tsubouchi, and H. Nakano, "A loop antenna with quasi-two sources for circular polarisation," *Electronics Letters*, vol. 58, no. 6, pp. 222–224, 2022.

[9] R. F. Harrington, *Fields Computation by Moment Methods*, Macmillan, New York, NY. USA, 1968.

[10] E. Baghernia, R. Movahedinia, and A. Sebak, "Broadband compact circularly polarized spiral antenna array fed by printed gap waveguide for millimeter-wave applications," *IEEE Access*, vol. 9, pp. 86–95, 2021.

[11] J. H. Richmond, "A wire-grid model for scattering by conducting bodies," *IEEE Transactions on Antennas and Propagation*, vol. 14, no. 6, pp. 782–786, 1966.

[12] N. Nguyentrong, S. J. Chen, and C. Fumeaux, "High-gain dual-band dual-sense circularly polarized spiral series-fed patch antenna," *IEEE Open Journal of Antennas and Propagation*, vol. 3, pp. 343–352, 2022.

[13] Y. Cao, S. Yan, J. Li, and J. Chen, "A pillbox based dual circularly-polarized millimeter-wave multi-beam antenna for future vehicular radar applications," *IEEE Transactions on Vehicular Technology*, vol. 71, no. 7, pp. 7095–7103, 2022.

[14] R. Li, G. DeJean, J. Laskar, and M. M. Tentzeris, "Investigation of circularly polarized loop antennas with a parasitic element for bandwidth enhancement," *IEEE Transactions on Antennas and Propagation*, vol. 53, no. 12, pp. 3930–3939, 2005.

[15] M. Sumi, K. Hirasawa, and S. Shi, "Two rectangular loops fed in series for broadband circular polarization and impedance matching," *IEEE Transactions on Antennas and Propagation*, vol. 52, no. 2, pp. 551–554, 2004.